Estimating Soil Water Contents from Soil Temperature Measurements by Using an Adaptive Kalman Filter

SHU-WEN ZHANG AND CHONG-JIAN QIU

Department of Atmospheric Science, Lanzhou University, Lanzhou, Gansu, China

QIN XU

National Severe Storms Laboratory, Norman, Oklahoma

(Manuscript received 18 November 2002, in final form 20 May 2003)

ABSTRACT

A simple soil heat transfer model is used together with an adaptive Kalman filter to estimate the daily averaged soil volumetric water contents from diurnal variations of the soil temperatures measured at different depths. In this method, the soil water contents are estimated as control variables that regulate the variations of soil temperatures at different depths and make the model nonbiased, while the model system noise covariance matrix is estimated by the covariance-matching technique. The method is tested with soil temperature data collected during 1–31 July 2000 from the Soil Water and Temperature System (SWATS) within the Oklahoma Atmospheric Radiation Measurement (ARM) central facilities at Lamont. The estimated soil water contents are verified against the observed values, and the rms differences are found to be small. Sensitivity tests are performed, showing that the method is reliable and stable.

1. Introduction

Soil moisture often plays a critical role in regulating small-scale and mesoscale moist processes, especially, when the vegetation cover and soil texture exhibit significant variability over these scales (Deardorff 1978; McCumber and Pielke 1981; Ek and Cuenca 1994). To date, there exists no simple and reliable method to estimate soil moisture on an operational basis (Ungar et al. 1992). For research purposes, however, different approaches were developed in recent years to estimate soil water content. For example, a first-order autoregressive Markovian model was formulated based on soil water transport and hydraulic budget to estimate soil water content and to compute the mean diffusivity of soil moisture (Parlange et al. 1992). Remotely sensed data were widely used to estimate water content (Starks and Jackson 2001; Mancini et al. 1999). Multiple-scale variations of surface soil moisture were also taken into consideration in hydraulic-budget studies and estimations (Parlange et al. 1993; Cahill et al. 1999; Montaldo and Albertson 2003). Aside from the previously mentioned hydraulic budget models, by using equations of an air–vegetation–soil layer coupled model as constraints, a variational method has been recently developed to compute sensible and latent heat fluxes from conventional observations obtained at meteorological surface stations (Zhou and Xu 1999, henceforth referred to as ZX99). As an extension of the method of Xu et al. (1999), this method can retrieve the top-layer soil water content and surface skin temperature as byproducts. The retrieved soil water content can be reliable only in daytime. The air–vegetation–soil layer coupled model used in Xu et al. (1999) and ZX99 is a diagnostic model that did not include the time dimension, so the time tendency information in the soil temperature measurements is not utilized. This leaves some opportunities for further improvements. Toward this end, a simple linear-regression method was developed by Xu and Zhou (2003) to retrieve daily averaged soil water content from diurnal variations of soil temperature measured at three or more depths. However, since the random part of the observation error was mixed into the random part of the equation error in their linear-regression equation, the total random error was large and not controlled. To improve the retrievals, it is necessary to model the random part of the equation error statistically (essentially the error covariance). This requires an advanced method, such as the adaptive Kalman filter (Mehra 1972). This is the motivation of this study.

In general, the soil temperature is assumed to obey a simple heat transfer equation (Hillel 1980; Koorevaar et al. 1983; Campbell 1985). In this equation there are

Corresponding author address: Dr. Qin Xu, National Severe Storms Laboratory, 1313 Halley Circle, Norman, OK 73069.
E-mail: Qin.Xu@noaa.gov

two important parameters: the soil heat capacity and thermal conductivity. For a given soil texture, the soil heat capacity and thermal conductivity depend mainly on the soil water content and are monotonic functions of soil water content. Since the soil water content changes very slowly over a day's period except for a heavy-rain day, the soil water content can be represented by its daily average in terms of its effects on the soil heat capacity, thermal conductivity, and the diurnal variations of soil temperature. For a given vertical distribution of soil water content on a day, the soil heat transfer equation can be integrated with the observed initial and boundary conditions to predict the diurnal variation of the vertical distribution of soil temperature. This is the forward problem. The associated inverse problem is to estimate the daily averaged vertical distribution of soil water content from observed diurnal variations of soil temperatures at different depths. Since there is no prior information about the model system noise (the random part of the system error) and this noise causes an uncertainty when the model is integrated in time, an adaptive Kalman filter (Mehra 1972) is constructed and used to deal with this uncertainty as well as random errors in the initial condition and observations in order to make good use of the available soil temperature observations. Because soil water contents are unknown parameters and the system noise is not known either, the covariance-matching technique (Mehra 1972) is used in this paper to estimate the statistics of the system noise. The model equation and method are described in the next section. Section 3 presents the results of the method applied to data collected by Soil Water and Temperature System (SWATS) at the Oklahoma Atmospheric Radiation Measurement Program–Cloud and Radiation Test Bed (ARM–CART) central station. The results are summarized with conclusions in section 4.

2. Model equation and method

a. Model equations

The vertical heat transfer process in the soil can be described by the following equation (Hillel 1980):

$$C(w)\frac{dT}{dt} = \frac{d}{dz}D(w)\frac{dT}{dz}, \quad (1)$$

where T is the soil temperature, w is the soil water content (measured by volume: $m^3\ m^{-3}$), $C(w)$ is the volumetric soil heat capacity, $D(w)$ is the soil thermal conductivity, and z is the vertical coordinate (distance from the surface, positive downward). The heat transfer process in the soil can be affected by plant roots, liquid water and water vapor movements, water phase changes and associated hysteresis in the soil (de Vries 1975; Milly 1982). The effects of these physical processes on heat transfer are often too complex to quantify and too subtle to detect, and so they are all neglected in (1). The soil heat capacity and thermal conductivity are functions of soil water content and soil texture. For the soil heat capacity, the function form is

$$C(w) = \rho_s c_s(1 - k_a) + \rho_w c_w w + \rho_a c_a(k_a - w), \quad (2)$$

where k_a is the soil porosity ($m^3\ m^{-3}$); ρ_s, ρ_w, and ρ_a are the densities; and c_s, c_w, and c_a are the specific heat capacities for soil, liquid water, and air, respectively. The value of $\rho_s c_s$ depends on the soil type (see Table 11-5 of Pielke 1984), $\rho_w c_w = 4.18 \times 10^6\ J\ m^{-3}\ K^{-1}$, and $\rho_a c_a = 1.2 \times 10^3\ J\ m^{-3}\ K^{-1}$. Because the air heat capacity is much smaller than the soil and water heat capacity, the term associated with the air heat capacity can be neglected and (2) reduces to

$$C(w) = \rho_s c_s(1 - w_s) + \rho_w c_w w, \quad (3)$$

where w_s $(=k_a)$ is the saturated soil volumetric water content. According to Al Nakshabandi and Kohnke (1965) and McCumber and Pielke (1981), the soil thermal conductivity ($m^{-1}\ K^{-1}$) can be related to w by the following empirical expression:

$$D(\psi) = \begin{cases} 418\ \exp(-\log_{10}|\psi| - 2.7) & \text{for } \log_{10}|\psi| \le 5.1 \\ 0.17 & \text{for } \log_{10}|\psi| > 5.1, \end{cases} \quad (4)$$

where ψ is the soil water potential representing the work required to extract water from the soil against capillarity and gravity (cm). It is defined by

$$\psi = \psi_s\left(\frac{w}{w_s}\right)^{-b}, \quad (5)$$

where ψ_s is the saturated soil water potential, and b is the pore size distribution index constant (Clapp and Hornberger 1978; also see Table 11-5 of Pielke 1984).

b. Discrete model and Kalman filter

The soil heat transfer equation is discretized by the finite-volume method (Versteeg and Malalasekera 1995). The vertical domain is divided into discrete control volumes with the grid points placed at the measurement depths, and so the modeled soil temperatures can be directly compared with the observed. In this method, each internal grid point is surrounded by a control volume whose boundaries are located halfway to the adjacent grid points. Thus, the soil temperature at each grid point represents the averaged value over its control volume and the heat fluxes are at the boundaries of the control volume. The soil heat transfer equation is then discretized into the following form:

$$\frac{C_i(T_i^n - T_i^{n-1})}{\Delta t} = 2\frac{(G_{i+1/2} - G_{i-1/2})}{(\Delta z_i + \Delta z_{i+1})}, \quad i = 2, 3, \ldots, m - 1, \quad (6)$$

where Δt is the time step, superscript n denotes the nth

time level, Δz_i is the vertical distance between the grid points z_i and z_{i-1}, m is the total number of measurement depths, and

$$G_{i-1/2} = D_{i-1/2}(T_i^n - T_{i-1}^{n-1})/\Delta z_i \quad \text{and} \tag{7}$$

$$G_{i+1/2} = D_{i+1/2}(T_{i+1}^{n-1} - T_i^n)/\Delta z_{i+1} \tag{8}$$

are the heat fluxes (positive upward: W m^{-2}) at $z_{i-1/2}$ and $z_{i+1/2}$, respectively.

For the data used in this paper, the measurement time interval is relatively large ($\Delta\tau = 1$ h as described in section 3a). To ensure the stability and accuracy of the time integration and to facilitate the Kalman filter formulation, a proper integer Δn (=12) is selected to give a sufficiently small value for $\Delta t = \Delta\tau/\Delta n$ (=300 s). Boundary values of T at points $i = 1$ and $i = m$ are given by the measurements and their linear interpolations (to the model time levels). Since the method used in (6)–(8) is locally implicit (Viterbo and Beljaars 1995) and the forward time level $n\Delta t$ is associated only with point i, the earlier difference equations can be written into the following vector form:

$$\mathbf{T}_n = \mathbf{F}\mathbf{T}_{n-1} + \mathbf{B}\mathbf{U}_{n-1}. \tag{9a}$$

Here, $\mathbf{F}$ is the model operator—a matrix of $(m-2)\times(m-2)$ whose elements are functions of the soil texture and soil water content, $\mathbf{T}_n$ is a vector of $m-2$ dimensions representing the soil temperature profile at time $n\Delta t$, $\mathbf{B}$ is the boundary forcing operator, which is an $(m-2)\times 2$ matrix, and $\mathbf{U}_{n-1}$ is a two-dimensional vector whose elements are given by the observed boundary values or their temporal interpolations at time $(n-1)\Delta t$. Integrating (9a) by Δn (=12) steps gives the following forward equation over one observation time interval $\Delta\tau = \Delta n\Delta t$:

$$\mathbf{T}_n = \mathbf{A}\mathbf{T}_{n-\Delta n} + \sum \mathbf{F}^{n'-1}\mathbf{B}\mathbf{U}_{n-n'}, \tag{9b}$$

where $\mathbf{A} = \mathbf{F}^{\Delta n}$ and the summation Σ is over n' from 1 to Δn.

The model system in (9b) is assumed to be unbiased but is not free of random errors. The true state vector evolves according to

$$\mathbf{T}_k^t = \mathbf{A}\mathbf{T}_{k-1}^t + \mathbf{B}_k + \mathbf{q}_k. \tag{10}$$

Here, $\mathbf{T}_k^t$ denotes the true state vector at $t = k\Delta\tau = k\Delta n\Delta t$, that is, the kth observation time level or, equivalently, the $k\Delta n$th model time level; $\mathbf{B}_k$ represents the last term in (9b), that is, $\Sigma\,\mathbf{F}^{n'-1}\,\mathbf{B}\mathbf{U}_{n-n'}$ with $n = k\Delta n$; and $\mathbf{q}_k$ is a random vector of $(m-2)$ dimensions representing the system noise at $t = k\Delta\tau$. The system noise takes account of errors in the model and boundary conditions.

As in the conventional Kalman filter (Jazwinski 1970), a predictive equation for the probabilistic mean of $\mathbf{T}_k^t$ can be derived from the statistical mean of (10). The result is

$$\mathbf{T}_k^f = \mathbf{A}\mathbf{T}_{k-1}^a + \mathbf{B}_k, \tag{11}$$

where $\mathbf{T}_k^f$ and $\mathbf{T}_k^a$ denote the predicted and analyzed state vectors at time $k\Delta\tau$, respectively. Denote by $\mathbf{P}_k^f$ and $\mathbf{P}_k^a$ the error covariance matrices associated with the state vectors $\mathbf{T}_k^f$ and $\mathbf{T}_k^a$, respectively. An equation for the error covariance propagation can be derived from the second-order statistical moment of the difference equation obtained by subtracting (11) from (10). The result is

$$\mathbf{P}_k^f = \mathbf{A}\mathbf{P}_{k-1}^a\mathbf{A}^{\mathrm{T}} + \mathbf{Q}_k, \tag{12}$$

where $\mathbf{Q}_k$ is the model system noise covariance matrix defined by the second-order statistical moment of $\mathbf{q}_k$ and $(\,)^{\mathrm{T}}$ denotes the transpose of $(\,)$. For simplicity, it is assumed in the derivation of (12) that $\mathbf{q}_k$ is not correlated in time and is independent of observation errors and, consequently, not correlated with errors in the analysis obtained at the previous $(k-1)$-th time level.

The observation vector, denoted by $\mathbf{Y}_k$, is related to the true state by

$$\mathbf{Y}_k = \mathbf{H}_k\mathbf{T}_k^t + \mathbf{e}_k = \mathbf{T}_k^t + \mathbf{e}_k, \tag{13}$$

where $\mathbf{H}_k$ is an $m_0 \times m$ matrix representing the observation operator and $\mathbf{e}_k$ is a vector of m_0 dimensions representing unbiased observation error at the kth time level. As mentioned earlier, the model grid is chosen to coincide with the measurement points to avoid interpolation errors, and so the observation matrix $\mathbf{H}_k$ reduces to a unit matrix of rank $(m-2)$, denoted by $\mathbf{I}$. This condition ($\mathbf{H}_k = \mathbf{I}$) is used in the second part of (13). The optimal analysis of the state vector is given by

$$\mathbf{T}_k^a = \mathbf{T}_k^f + \mathbf{K}_k(\mathbf{Y}_k - \mathbf{T}_k^f), \tag{14}$$

where $\mathbf{H}_k = \mathbf{I}$ is used, $\mathbf{K}_k$ is the Kalman gain defined by

$$\mathbf{K}_k = \mathbf{P}_k^f(\mathbf{P}_k^f + \mathbf{R}_k)^{-1}, \tag{15}$$

and $\mathbf{R}_k$ is the observation error covariance, an $m_0 \times m_0$ matrix, at the kth time level defined by the second-order statistical moment of $\mathbf{e}_k$. As the error is reduced in the analysis, the analysis error covariance matrix is updated by

$$\mathbf{P}_k^a = (\mathbf{I} - \mathbf{K}_k)\mathbf{P}_k^f. \tag{16}$$

Integrating the preceding equations requires $\mathbf{Q}_k$ and $\mathbf{R}_k$ be known at each time level and the initial values $\mathbf{T}_0^a$ and $\mathbf{P}_0^a$ be given. The specifications of these matrices and related assumptions are described as follows.

1) SYSTEM NOISE COVARIANCE $\mathbf{Q}_k$

The system noise includes all unknown influences. It is the collection of random errors due to all simplifications and assumptions made in the model as well as the uncertainties in the parameters (such as the soil heat capacity and thermal conductivity) and the boundary conditions. In this paper, the system noise is assumed to be a multidimensional Gaussian white process and thus, can be completely characterized by the mean value and covariance matrix. Consequently, if a model is not

biased, the mean value of the system noise will be zero. Because the system noise represents all influences not modeled for the given time level, its covariance matrix $\mathbf{Q}_k$ is a measure of the uncertainty of the model. Its elements can be regarded as parameters belonging to the model. These elements will be called the stochastic parameters (Van Geer et al. 1991), to distinguish them from the soil parameters in the matrices **A** and **B**, which can be interpreted physically as the variability of the system. Depending on the dimension of the model variable space versus the dimension of the observation variable space, various approaches have been developed to calculate the system noise covariance (Cahill et al. 1999; Cane et al. 1996; Van Geer et al. 1991). In this study, however, the dimensions of the two spaces are not only equal but also very small, and so the covariance-matching technique can be used directly [see (21)].

2) Observation error covariance $\mathbf{R}_k$

The observation errors are assumed to be zero-mean, noncorrelated, and independent of the system noise, so $\mathbf{R}_k$ reduces to $\sigma^2\mathbf{I}$ where σ^2 is the observation error variance. The observation errors are generally very small in comparison with the other sources of uncertainty, and $\sigma^2 = 0.001$ K^2 is used in this paper (see section 3b).

3) Initial values $\mathbf{T}_0^a$ and $\mathbf{P}_0^a$

Because the influence of these initial values will diminish gradually, it does not matter much whether those two initial values can be precisely given. In this paper, $\mathbf{T}_0^a$ is given by the observation and $\mathbf{P}_0^a$ is simply set to be the same as $\mathbf{R}_k = \sigma^2\mathbf{I}$ at the initial time $t = 0$.

c. Adaptive Kalman filter and covariance matching

The parameters to be estimated are the daily averaged soil water contents at the m different depths (contained in the matrices **A** and **B**) and the stochastic parameters (contained in the matrix $\mathbf{Q}_k$). During the estimation time window, the system noise covariance matrix $\mathbf{Q}_k$ is assumed to be constant, and so $\mathbf{Q}_k$ can be denoted by **Q**. Besides, a fixed measurement strategy ($\mathbf{H}_k = \mathbf{I}$ and $\mathbf{R}_k = \sigma^2\mathbf{I}$) holds. As the influence of the initial condition diminishes, all covariance matrices become independent of time. With these assumptions, the soil water contents and the stochastic parameters can be estimated as follows.

1) Soil water contents

It is known from Kalman filter theory that the innovation sequence produced by an optimal filter should be Gaussian white noise with a zero mean, while the innovation is a vector defined by

$$\mathbf{v}_k = \mathbf{Y}_k - \mathbf{H}_k\mathbf{T}_k^f = \mathbf{Y}_k - \mathbf{T}_k^f, \tag{17}$$

where $\mathbf{H}_k = \mathbf{I}$ is used. This implies that for an unbiased model the soil water contents can be estimated by adjusting their values to minimize the absolute value of each component of the sample mean of the innovation sequence vectors calculated by

$$\bar{\mathbf{v}} = \left(\frac{1}{N}\right)\sum_k \mathbf{v}_k, \tag{18}$$

where the summation Σ_k is from $k = 1$ to N while N is the total number of observation time levels for the 1-day period of the estimation time window.

2) Stochastic parameters

The system noise statistics are difficult to estimate in most practical situations. Incorrect a priori statistics in the design of a Kalman filter can lead to large estimation errors or even to a divergence of errors. The covariance-matching technique is a very useful method to tackle this problem as it can estimate the statistics of system noises from the observed soil temperatures. The basic idea behind the covariance-matching technique is to make the residuals consistent with their theoretical covariance (Mehra 1972). For an optimal filter, the innovation sequence vector $\mathbf{v}_k$ should have the following theoretical covariance:

$$\mathbf{X} = \mathbf{P}^f + \mathbf{R}, \tag{19}$$

where $\mathbf{H}_k = \mathbf{I}$ is used. If the actual covariance of $\mathbf{v}_k$ is much larger (measured by the absolute norm) than the theoretical covariance **X**, then the system noise **Q** should be increased. This has the effect of increasing $\mathbf{P}^f$ and bringing the actual covariance of $\mathbf{v}_k$ closer to **X**. The actual covariance of $\mathbf{v}_k$ is approximated by its sample covariance:

$$\mathbf{S} = \left(\frac{1}{N}\right)\sum_k (\mathbf{v}_k - \bar{\mathbf{v}})(\mathbf{v}_k - \bar{\mathbf{v}})^{\mathrm{T}}, \tag{20}$$

where the summation Σ_k is as in (18) and $(\,)^{\mathrm{T}}$ denotes the transpose of ( ). An equation for **Q** is obtained by setting $\mathbf{X} = \mathbf{S}$, which gives

$$\mathbf{S} = \mathbf{A}\mathbf{P}^a\mathbf{A}^{\mathrm{T}} + \mathbf{Q} + \mathbf{R}. \tag{21}$$

Since **H** is set to a unit matrix of rank $(m - 2)$, (21) can give a unique solution for **Q**. However, since the true value of **Q** is unknown, the computed $\mathbf{P}^f$ and $\mathbf{P}^a$ may not represent the actual error covariances. Because of this, the stochastic parameters have to be calibrated until the sample covariance matrix **S** does not differ significantly from the Kalman filter covariance matrix **X**. On the other hand, the sample mean in (18) and sample covariance matrix in (20) both depend on the estimated soil water contents as well as **Q**. Hence, the soil water contents and **Q** have to be estimated itera-

TABLE 1. Means and standard deviations of hydraulic parameters in (5) for three types of soil texture at six measurement depths.

Depth (cm)	Class	b		Ψ_s		w_s	
		Mean	Std dev	Mean	Std dev	Mean	Std dev
5, 15	Silt loam	5.30	1.72	78.6	2.4	0.485	0.054
25	Clay	11.40	3.93	40.5	3.9	0.482	0.035
35, 60, 85	Clay loam	8.52	3.74	63.0	5.2	0.476	0.054

tively. The iterative procedure consists of the following four basic steps:

Step 1. Start with a first guess of the system noise covariance matrix, say, given by $q_{ij}^{(0)} = 0.01 \exp(-0.28\Delta z_{ij})$ where $q_{ij}^{(0)}$ is the ijth element of $\mathbf{Q}^{(0)}$ and Δz_{ij} is the vertical distance between the ith and jth grid points, and with a first guess of the soil water content vector, denoted by $\mathbf{w}^{(0)}$ and given, for example, by the wilting-point values. Integrate (11) and (12) forward with $\mathbf{P}_k^a$ updated by (16).

Step 2. Substitute the computed $\mathbf{T}_k^f$ and the observation $\mathbf{Y}_k$ into (17)–(18) to compute the innovation sample mean. The result is denoted by $\overline{\mathbf{v}}^{(0)}$. If an element of $\overline{\mathbf{v}}^{(0)}$ is larger (or smaller) than zero, then the corresponding element of $\mathbf{w}^{(0)}$ is adjusted by a small percentage (3%) increase (or decrease). If the adjusted element is adjacent to one of the two boundary points, then the element at the two boundary point is also adjusted by the same percentage. Use this adjusted vector, denoted by $\mathbf{w}^{(1)}$, in place of $\mathbf{w}^{(0)}$ to repeat the integration of (11) and (12) in step 1 and recalculate the innovation sample mean $\overline{\mathbf{v}}^{(1)}$.

Step 3. Denote by $w_i^{(0)}$ and $\overline{v}_i^{(0)}$ the ith components of $\mathbf{w}^{(0)}$ and $\overline{\mathbf{v}}^{(0)}$, respectively, and by $w_i^{(1)}$ and $\overline{v}_i^{(1)}$ the ith components of $\mathbf{w}^{(1)}$ and $\overline{\mathbf{v}}^{(1)}$, respectively. Denote by $[w_i^{(2)}, 0]$ the zero point of the linear function that passes through the ith pair of points: $[w_i^{(0)}, \overline{v}_i^{(0)}]$ and $[w_i^{(1)}, \overline{v}_i^{(1)}]$. Calculate $w_i^{(2)}$ by linear interpolation. Use the vector composed of $w_i^{(2)}$, that is, $\mathbf{w}^{(2)}$ in place of $\mathbf{w}^{(1)}$ to repeat the integration in step 1 and recalculate the innovation sample mean $\overline{\mathbf{v}}^{(2)}$ in step 2. Use the L_1 norm defined by $\|\overline{\mathbf{v}}^{(0)}\|_1 = \Sigma_i |\overline{v}_i^{(0)}|$ as a measure of smallness of $\overline{\mathbf{v}}^{(0)}$, where the summation Σ_i goes through all the internal grid points. If $\|\overline{\mathbf{v}}^{(0)}\|_1 \geq \|\overline{\mathbf{v}}^{(1)}\|_1$ (or $\|\overline{\mathbf{v}}^{(0)}\|_1 < \|\overline{\mathbf{v}}^{(1)}\|_1$), then pair $\mathbf{w}^{(2)}$ with $\mathbf{w}^{(1)}$ [or $\mathbf{w}^{(0)}$] to repeat the linear interpolation and related procedures until the absolute norm of the innovation sample mean reaches a minimum. This completes an inner loop of the iterations, and the procedure enters an outer loop in step 4.

Step 4. In the above procedure, $\mathbf{P}_k^a$ is updated by (16) and becomes stationary as soon as $k > 2$. Thus, $\mathbf{P}_k^a$ can be denoted by $\mathbf{P}^a$ and substituted into (21), while $\mathbf{S}$ is computed from (20) by using $\mathbf{v}_k$ computed in step 3. The system noise covariance matrix is then estimated from (21) and denoted by $\mathbf{Q}^{(1)}$. The difference between $\mathbf{Q}^{(1)}$ and $\mathbf{Q}^{(0)}$ is measured by the L_1 norm: $\|\mathbf{Q}^{(1)} - \mathbf{Q}^{(0)}\|_1 = \max_j \Sigma_i |q_{ij}^{(1)} - q_{ij}^{(0)}|$. If $\|\mathbf{Q}^{(1)} - \mathbf{Q}^{(0)}\|_1 \leq 10^{-4}$, then the estimated $\mathbf{Q}^{(1)}$ is acceptable and the outer loop of the iterations is completed and so is the entire iterative procedure. Otherwise, replace $\mathbf{Q}^{(0)}$ by $\lambda\mathbf{Q}^{(1)} + (1 - \lambda)\mathbf{Q}^{(0)}$ and return to step 3, where λ is between 0 and 1.

When the above procedure is applied to real data (see the next section), the system noise covariance matrix estimated by the covariance-matching technique often undergoes strong variations in the first few outer loops. In this case, the estimated $\mathbf{Q}$ from (21) does not represent the real covariance matrix. To prevent the divergence, λ should be less than 1 and $\lambda = 0.6$ is used in this paper. Without precipitation, the soil water contents change slowly and thus the estimated values for the previous day can be used as an initial guess for the next day. In this case, the iterative procedure will converge quickly. For the first day or a rainy day, however, there is no such good first guess, and so the procedure takes a relatively large number of iterations to converge. Nevertheless, because the daily variations of soil water contents are not large and the number of the grid points is small, the iterative procedure never fails to converge for the case presented in the next section.

3. Applications

a. Description of the data

The data used in this paper were collected hourly at two (east and west) sites within the Oklahoma ARM–CART central facilities at Lamont during 1–31 July 2000. These two sites are only 1 m apart from each other and are both located under pasture on a broad hilltop, where the soil texture changes with depth gradually from silt loam in the surface layer, to clay in the middle layer, and to clay loam in the bottom layer (see the first two columns of Table 1). Below the bottom layer, a layer of sandstone begins at the depth of 88 cm.

The weather was not calm during July 2000 and heavy rainfalls were recorded on 2, 11, 21, and 27 July by the ARM–CART central facilities at Lamont. In summer 2000, a new calibration was developed for each SWATS to ensure proper measurements for wet soil. During July, the soil at Lamont two times experienced sudden wetting (due to heavy rainfalls) and then gradual drying processes. As the soil water contents changed a great deal, the data collected over this month should represent a

TABLE 2. Estimated system noise variances (Var) and innovation sample means ($\bar{\mathbf{v}}$) with two different settings of σ^2 on a typical rainy day (4 Jul 2000).

Depth (cm)	$\sigma^2 = 0.001$ (East)		$\sigma^2 = 0.003$ (East)		$\sigma^2 = 0.001$ (West)		$\sigma^2 = 0.003$ (West)	
	Var	$\bar{\mathbf{v}}$	Var	$\bar{\mathbf{v}}$	Var	$\bar{\mathbf{v}}$	Var	$\bar{\mathbf{v}}$
15	0.0017	−0.033	0.0009	−0.034	0.0251	0.029	0.0238	0.034
25	0.0015	0.048	0.0003	0.061	0.0093	−0.117	0.0080	−0.107
35	0.0046	−0.003	0.0034	0.009	0.0014	0.058	0.0009	0.097
60	0.0037	−0.051	0.0028	−0.064	0.0015	−0.079	0.0004	−0.139

broad range of situations and, thus, was selected for study.

At each site, a Soil Water and Temperature System (SWATS) was installed to measure both soil temperature and soil water at the depths of 5, 15, 25, 35, 60, and 85 cm using the Campbell Scientific 229-L heat dissipation matric potential sensors (Reece 1996) arrayed vertically into the soil. The twin profiles at the two sites provided operational redundancy, as well as an indication of spatial variability over 1-m horizontal separation. To assess the quality and accuracy of SWATS soil water measurements, Schneider et al. (2003) compared the SWATS measurements with those sampled by the benchmark oven-drying method. The assessed accuracy was about 0.05 $m^3\ m^{-3}$ in terms of rms error. Since 132 benchmark measurements were sampled within 5 m of the SWATS instruments for the comparison, their assessed rms error (0.05 $m^3\ m^{-3}$) included both the measurement error and sampling error. When the SWATS soil water data are used in this paper to verify the estimated soil water contents, which are the control-volume averaged values (see section 2b), the data also contain both (measurement and sampling) types of error. The total observation (measurement plus sampling) error could be very close to the value (0.05 $m^3\ m^{-3}$) assessed by Schneider et al. (2003).

The soil temperatures were measured accurately within 0.1 K by SWATS thermocouples. Note that the observation operator has been set to an unit matrix ($\mathbf{H}_k = \mathbf{I}$) in sections 2b,c. This means that the input soil temperatures are treated as the control-volume averaged values, so they contain both types of error (measurement and sampling). The sampling error could be much smaller than the measurement error provided the spatial variations of soil temperature were very small within a control volume. Since no information is available to quantify the sampling error, in the next section the observation error variance in the adaptive Kalman filter will be specified purely based on the instrument accuracy.

b. Sensitivity tests

It is assumed in (13) that the temperature observation errors are random and unbiased. Small biases in the temperature observations were possible, but they should have nearly no impact on the estimated soil water contents. As indicated by (6) and (7), the soil water contents are related to the temporal and spatial differences of soil temperature which are insensitive to biases in the soil temperature observations (as the biases are largely eliminated by differencing). This explains why small biases in the temperature observations can be neglected (also as verified by our numerical experiment not shown in this paper). Thus, only the random part of the temperature observation errors will be considered for the sensitivity tests in this section.

Because the soil temperatures were measured by the thermocouple automatically at each SWATS site and the thermocouple is stable and accurate to 0.1 K, the standard deviation of measurement errors should be about 0.05 K or smaller. Since the sampling error can be neglected (as explained in the previous section), the observation error variance σ^2 should be close to 0.001 K^2 or, at least, smaller than 0.003 K^2. Numerical experiments are performed to examine the sensitivities of the estimates to the variation of σ^2 from 0.001 to 0.003 K^2. It is found that the variation of σ^2 affects the estimated $\mathbf{Q}$ and $\bar{\mathbf{v}}$ but has almost no influence on the estimated soil water contents. The estimated system noise variances (that is, the four diagonal elements of $\mathbf{Q}$) and innovation sample means (that is, the four elements of vector $\bar{\mathbf{v}}$) obtained with the two different settings of $\sigma^2 = 0.001$ and 0.003 K^2 are listed in Table 2 for a typical rainy day (the 4th) and in Table 3 for a typical dry day (the 18th) during July 2000. In each table, the four col-

TABLE 3. As in Table 2 but for a typical dry day (18 Jul 2000).

Depth (cm)	$\sigma^2 = 0.001$ (East)		$\sigma^2 = 0.003$ (East)		$\sigma^2 = 0.001$ (West)		$\sigma^2 = 0.003$ (West)	
	Var	$\bar{\mathbf{v}}$	Var	$\bar{\mathbf{v}}$	Var	$\bar{\mathbf{v}}$	Var	$\bar{\mathbf{v}}$
15	0.0082	−0.024	0.0069	−0.029	0.0154	0.010	0.0107	0.016
25	0.0079	0.067	0.0067	0.069	0.0094	−0.083	0.0081	−0.074
35	0.0109	0.028	0.0095	0.033	0.0028	0.043	0.0018	0.075
60	0.0088	−0.037	0.0075	−0.041	0.0019	−0.070	0.0008	−0.107

TABLE 4. Differences between the observed and estimated soil water contents with three different settings of hydraulic parameters on a typical rainy day (4 Jul 2000).

	Errors for the east site			Errors for the west site		
Depth	Case 1	Case 2	Case 3	Case 1	Case 2	Case 3
5 cm	0.007	−0.013	−0.003	−0.015	−0.015	−0.005
15 cm	0.015	−0.005	0.015	−0.033	−0.033	−0.023
25 cm	−0.006	0.004	0.015	−0.025	−0.025	−0.025
35 cm	−0.017	−0.002	−0.017	−0.010	0.020	0.010
60 cm	−0.008	−0.003	−0.008	−0.013	−0.003	−0.003
85 cm	0.025	0.005	0.005	0.031	0.001	0.011
Rms	0.015	0.006	0.012	0.023	0.020	0.015

umns on the left side are for the east site and the four columns on the right side are for the west sites. As shown by the Tables 2 and 3, the estimated system noise variances are moderately sensitive to σ^2 but the innovation sample means are not very sensitive to σ^2. The estimated soil water contents have nearly the same values for the two different settings of σ^2, and so they are not listed in Tables 2 and 3 (but are plotted in Figs. 1 and 2 for $\sigma^2 = 0.001$).

Note that $\mathbf{R} = \sigma^2\mathbf{I}$ is used in (21) to adjust the estimated $\mathbf{Q}$ in the outer loop of the iterative procedure (see step 4 described in section 2c), and so the estimated $\mathbf{Q}$ is directly affected by the setting of σ^2. On the other hand, during each iteration the estimated soil water contents are adjusted to minimize $\bar{\mathbf{v}}$ in the inner loop of the iterative procedure (see step 3 described in section 2c). The minimized $\bar{\mathbf{v}}$ can only be indirectly affected by the setting of σ^2. This may explain why the estimated system noise variances are more sensitive to σ^2 than the innovation sample means as shown in Tables 2 and 3 and why the estimated soil water contents are insensitive to σ^2. When σ^2 decreases below 0.001 K^2, the estimated system noise variances and innovation sample means both become nearly independent of σ^2 (not shown). Based on this result and on the aforementioned accuracy and stability of the soil temperatures measured by the thermocouple, $\sigma^2 = 0.001$ K^2 can be used for the applications of the adaptive Kalman filter to the ARM–CART data (see section 3c). Once σ^2 is properly determined, the following criterion

$$|v_i^k| \le c(P_{ii^k}^f + \sigma^2)^{1/2} \tag{22}$$

can be used to control the quality of the input soil temperature data, where v_i^k is the ith element of the innovation vector $\mathbf{v}_k$, $P_{ii^k}^f$ is the ith diagonal element of matrix $\mathbf{P}_k^f$, and c is an empirical constant in the range from 3 to 4. Under this criterion, each soil temperature measurement, say, at the ith depth and kth observation time level should yield a sufficiently small value of v_i^k to satisfy (22). Otherwise, the temperature measurement is rejected and the associated innovation is not used in the statistics (Jia and Zhu 1984).

In addition to the observation errors, uncertainties in the values of the hydraulic parameters in (5) may also affect the estimates. The mean values of the three hydraulic parameters in (5) are listed in Table 1, which are quoted from Table 11-5 of Pielke (1984). According to the U.S. Department of Agriculture (USDA) soil texture classification, the physical properties are not unique for each soil textural class. Based on detailed analyses of 1448 samples of different soil textures, Cosby et al. (1984) assessed the standard deviations of the hydraulic parameters. For the aforementioned three types of soil textures, the assessed standard deviations are listed in Table 1. Using the values listed in Table 1, sensitivity experiments are performed with different settings of ψ_s, w_s, and b in the following three cases:

Case 1: Each hydraulic parameter is set to its mean value plus standard deviation.
Case 2: Each hydraulic parameter is set to its mean value minus standard deviation.
Case 3: Each hydraulic parameter is set to its mean value.

The differences between the observed and estimated soil water contents are listed in Table 4 for the above three

TABLE 5. As in Table 4 but for a typical dry day (18 Jul 2000).

	Errors for the east site			Errors for the west site		
Depth	Case 1	Case 2	Case 3	Case 1	Case 2	Case 3
5 cm	0.023	−0.007	−0.007	−0.010	0.005	0.010
15 cm	0.023	0.003	0.003	−0.034	−0.024	−0.014
25 cm	0.027	0.007	0.007	−0.025	−0.025	−0.025
35 cm	−0.021	−0.011	−0.011	−0.016	0.014	0.004
60 cm	−0.013	−0.003	−0.003	−0.024	−0.014	−0.014
85 cm	0.016	0.006	0.006	0.029	0.004	0.019
Rms	0.021	0.007	0.007	0.024	0.017	0.016

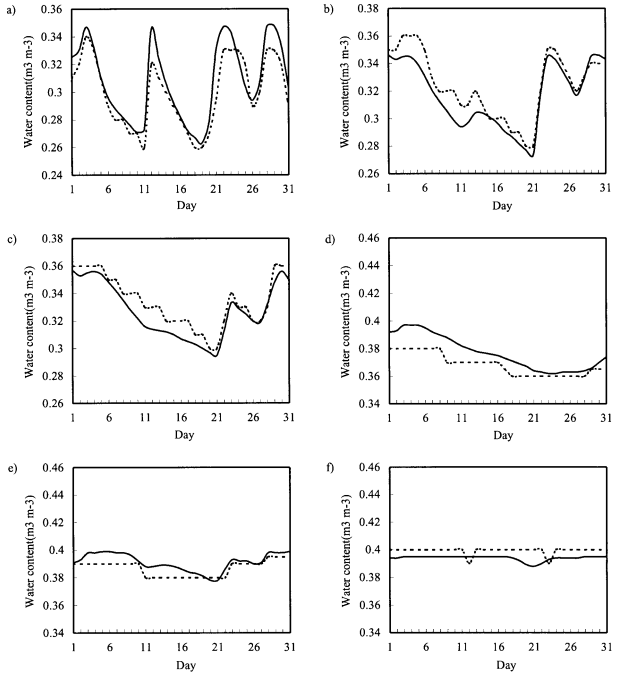

FIG. 1. Comparisons between the estimated (dashed) and directly measured (solid) soil volumetric water contents at depths of (a) 5, (b) 15, (c) 25, (d) 35, (e) 60, and (f) 85 cm for the east site.

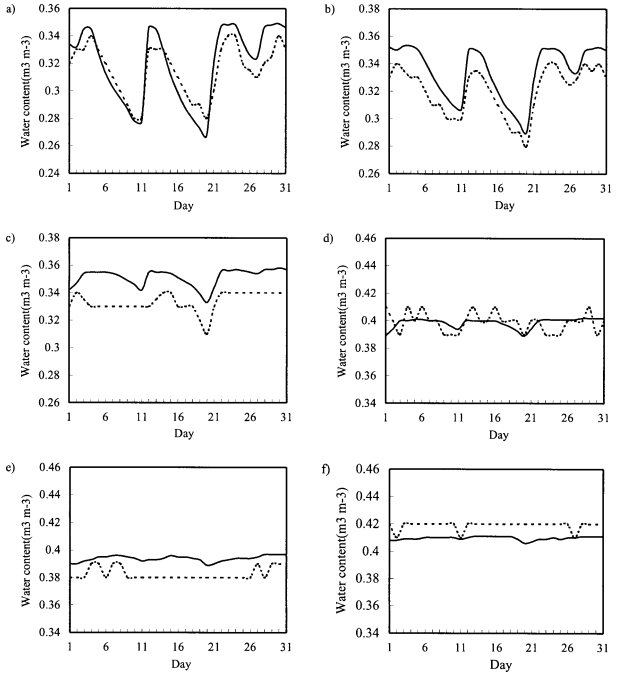

FIG. 2. As in Fig. 1 but for the west site.

cases of experiments performed for a typical rainy day (4 July). Table 5 is the same as Table 4 but is for a typical dry day (18 July). The results in these two tables indicate that the estimated soil water contents are moderately sensitive to the variations of ψ_s, w_s, and b in the ranges of their respective standard deviations. In case 1 (or case 2) all three hydraulic parameters are changed simultaneously by adding (or subtracting) their respective standard deviations to represent perhaps the worst situation. In practice, errors are rarely as large as these standard deviations simultaneously considered in all three hydraulic parameters. Thus, when the three hydraulic parameters are given by the respective mean values (as in case 3 and next section), possible errors in these mean values are unlikely to be simultaneously as large as their respective standard deviations and thus should not seriously deteriorate the accuracy of the estimated soil water contents.

c. Results and discussion

The estimates of the daily averaged soil volumetric water contents at the two sites are plotted in Figs. 1 and 2 against the observations at the depths of 5, 15, 25, 35, 60, and 85 cm. As shown, the estimated soil water contents (shaded curves) are close to the observed values (solid curves) at each site. The differences between the estimated and observed values are slightly smaller at the east site than those at the west site. At the east site, the differences (estimated minus observed) are generally negative at the depths of 5, 35, and 60 cm (Figs. 1a,d,e) and are generally positive at the depths of 15, 25, and 85 cm (Figs. 1b,c,f). At the west site, the differences are generally negative at the depths of 15, 25, and 60 cm (Figs. 2b,c,e), are generally positive at the depth of 85 cm (Fig. 2f), and change signs many times

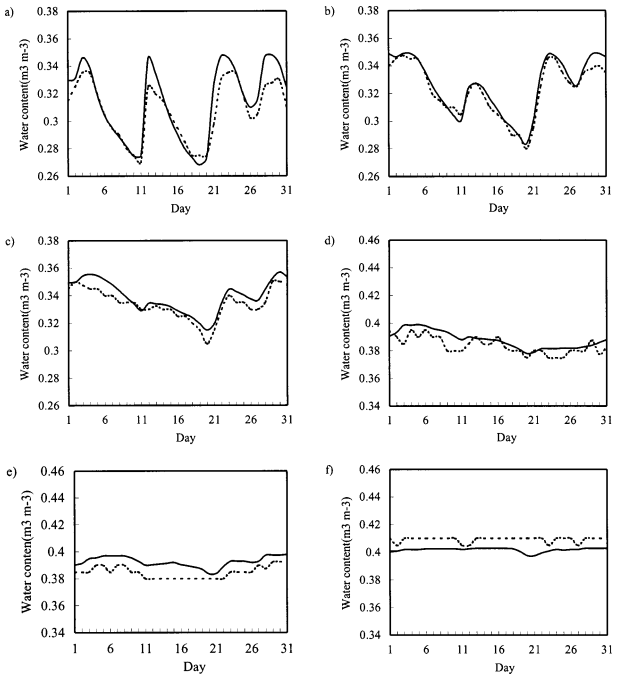

FIG. 3. As in Fig. 1 but averaged for the two sites.

TABLE 6. The rms differences between the estimated and observed soil water contents (first three columns) and between the observed soil water contents at two sites (last column).

Depth	Rms difference			Rms difference between the observed
	East	West	Avg	
5 cm	0.013	0.013	0.011	0.018
15 cm	0.010	0.015	0.005	0.024
25 cm	0.009	0.018	0.006	0.030
35 cm	0.010	0.008	0.006	0.025
60 cm	0.006	0.012	0.008	0.006
85 cm	0.006	0.010	0.008	0.016
Avg	0.009	0.013	0.007	0.020
Percentage	2.62%	3.54%	2.11%	5.56%

at the depths of 5 and 35 cm (Figs. 2a,d). The two-site averaged estimates are plotted in Fig. 3 against the two-site averaged observations. In comparison with the results at each individual site in Figs. 1–2, the differences between the two-site averaged estimates and observations are clearly smaller than those at each individual site.

The rms differences between the estimated and observed soil water contents are listed in the first three columns of Table 6 for the east site, west site and two-site averaged case, respectively. The first six rows are for the six depths, the seventh row is for the six depth-averaged values, and the last row is for the relative rms differences given by the percentages of the values in the seventh row with respect to the six depth-averaged rms values of the observed soil water contents. The relative rms difference is 2.11% for the two-site averaged case, which is smaller than that (2.62%) for the east site, while the latter is smaller than that (3.54%) for the west site. The rms differences listed in the seven rows of the first three columns are smaller than the observation error (0.05 $m^3\ m^{-3}$). This and the smallness of the relative rms differences indicate that the estimated soil water contents are quite accurate.

The rms differences between the observed soil water contents at the two sites are listed in the last column of Table 6. These rms differences are still smaller than the observation error (0.05 $m^3\ m^{-3}$) but are larger than the rms differences between the estimated and observed soil water contents in the first three columns. Thus, a certain degree of soil water content heterogeneity existed between the two sites but it could not be well quantified by the SWATS measurements. Note that the averaged rms difference for the two-site averaged case is 0.007, which is smaller than that (0.009 or 0.0013) for each individual site, while the latter is smaller than the averaged rms difference (0.02) between the observed soil water contents at the two sites. This suggests that the method has an improved skill when it is used to estimate area-averaged soil water contents from soil temperature measurements at two or more sites.

Although the estimated soil water contents are quite accurate in general, they do not reach the peak values measured in the shallow near-surface soil layer on the four rainy days (2, 11, 21, and 27 July), as shown in Figs. 1a,b and 2a,b. The near-surface soil layer was dry on the day before each of these rainy days. During each of these rainy days, the water movement caused by infiltrated rainfall could become significant and no longer be neglected especially in the near-surface soil layer (Cahill and Parlange 1998). This heavy rain-caused process, however, is neglected by the soil heat transfer equation [(1)] as mentioned in section 2a, and so the equation becomes inaccurate or even invalid in this case. The adaptive Kalman filter, however, still converges and estimates the soil water contents reasonably well on these rainy days. This is because the adaptive Kalman filter can adjust the estimated soil water contents and thus adjust the modeled soil thermal conductivity to fit the effective thermal conductivity implied by the observations that have included the influence of water movement. In this case, the modeled thermal conductivity should represent the effective thermal conductivity rather than the one modeled by (4)–(5) in this paper. However, the soil water content cannot be accurately estimated as it is related to the thermal conductivity by the simple soil heat transfer equation [(1)] in the current model. This may partially explain why the estimated soil water contents cannot reach the peak values measured in the shallow soil layer on the heavy-rain days. Furthermore, according to Peters-Lidard et al. (1998) who studied the thermal conductivity data collected in the First International Satellite Land Surface Climatology Project (ISLSCP) Field Experiment (FIFE), the formulation (4) used in section 2a tends to overestimate soil thermal conductivity during wet periods. Thus, the approximations involved in (4) could also be partially responsible for the differences between the estimated and observed soil water contents, especially on the heavy-rain days. Peters-Lidard et al. (1998) proposed an improved formulation to replace (4), but it contains additional parameters (particularly quartz content) whose values and related specifications are not available for the two sites considered in this paper. Using the improved formulation to replace (4) is subject to future studies.

4. Summary and conclusions

In this paper, the adaptive Kalman filter with the covariance-matching technique is applied to a soil heat transfer model to estimate the daily averaged soil water contents from observed soil temperatures at the same depths. In the soil heat transfer model, the soil thermal conductivity is related to the soil water content, and so the latter can be estimated as a control vector from the observed diurnal variations of the soil temperatures at different depths. By applying the adaptive Kalman filter to the model, the vertical profile (represented by a vector) of the soil temperature is integrated forward to-

gether with its error covariance matrix between observation times, while the optimal interpolation is performed at every observation time. The model is assumed to be unbiased or can be made unbiased by adjusting the control vector that represents the soil water contents at the depths of temperature observations. If this control vector and the model system noise covariance matrix are accurately estimated, then the time series of innovation (observed minus model-integrated) vectors should be noncorrelated in time with zero mean, and the innovation covariance matrix should match its theoretical estimate [see (20)–(21)]. An iterative procedure is designed to adjust the control vector and system noise covariance matrix so that the above two statistical properties discussed earlier can be satisfied to a certain accuracy.

The method is tested with soil temperature and soil water content measurements collected at two SWATS sites within the Oklahoma ARM–CART central facilities for the entire month of July 2000. In particular, sensitivity experiments are performed with different settings of observation error variance σ^2 and different settings of possible values in the three hydraulic parameters in (5). The results show that varying σ within the range of the instrument accuracy and stability affects the estimated system noise variances moderately and influences the innovation sample means slightly (see Tables 2 and 3), but has nearly no impact on the estimated soil water contents. In this paper, σ is determined based on the instrument accuracy and stability. With a properly determined σ, large outlays in the innovation vector can be detected [see (22)] and thus used to control the quality of the input soil temperature data. However, the estimated soil water contents are found to be moderately sensitive to the variations of hydraulic parameters in the ranges of their respective standard deviations given by Cosby et al. (1984), at least for the three types of soil textures (silt loam, clay, and clay loam) at the two sites considered in this paper (see Tables 4 and 5).

The estimated soil water contents are close to the observed and their rms differences are smaller than the observation error (0.05 $m^3\ m^{-3}$). The averaged rms difference is a small percentage of the averaged rms value of the observed soil water contents at each site: 2.62% for the east site, 3.54% for the west, and merely 2.11% for the two-site averaged case (see Table 6). While the estimated soil water contents are quite close to the observed, relatively large rms differences are seen in the shallow layer (at the depths of 5 and 15 cm). In particular, the estimated soil water contents cannot reach the peak values measured in the shallow soil layer on the heavy-rain days (see Figs. 1a,b and 2a,b). The soil heat transfer equation is relatively simple [see (1)] and does not consider the heavy-rain-caused water movement in the soil. This could be a major source of error for the underestimated soil water contents on the heavy-rain days, as explained in section 3c.

Measuring soil temperature is more convenient and less expensive than measuring soil water content. The method developed in this paper provides a useful tool to estimate soil water content from soil temperature measurements, and the method is shown to be quite accurate and reliable, at least, for the case tested in this paper. When soil temperature measurements are available at two or more sites over a small area, area-averaged soil water contents are expected to be even better estimated by the method (as suggested by the results in Table 6).

Acknowledgments. The authors are thankful to Kang Nai at the University of Oklahoma for data preparations. The data were kindly provided by the Atmospheric Radiation Measurement (ARM) Program. Comments and suggestions from Dr. Jeff Basara at the University of Oklahoma and anonymous reviewers improved the presentation of the results. The first two authors acknowledge the support by Chinese NSF Grant E-D0119-90202014 to Lanzhou University.

REFERENCES

Al Nakhabandi, G., and H. Kohnke, 1965: Thermal conductivity and diffusivity of soil as related to moisture tension and other physical properties. *Agric. Meteor.,* **2,** 271–279.

Cahill, A. T., and M. B. Parlange, 1998: On water vapor transport in field soils. *Water Resour. Res.,* **34,** 731–739.

——, F. Ungaro, M. B. Parlange, M. Mata, and D. R. Nielsen, 1999: Combined spatial and Kalman filter estimation of optimal soil hydraulic properties. *Water Resour. Res.,* **35,** 1079–1088.

Campbell, G., 1985: *Soil Physics with Basic-Transport Models for Soil-Plant Systems.* Elsevier, 150 pp.

Cane, M. A., A. Kaplan, R. N. Miller, B. Tang, E. C. Hackert, and A. J. Busalacchi, 1996: Mapping tropical Pacific sea level: Data assimilation via a reduced state space Kalman filter. *J. Geophys. Res.,* **101,** 22 599–22 617.

Clapp, R. B., and G. M. Hornberger, 1978: Empirical equations for some soil hydraulic properties. *Water Resour. Res.,* **14,** 601–604.

Cosby, B. J., G. M. Hornberger, R. B. Clapp, and T. R. Ginn, 1984: A statistical exploration of the relationships of soil moisture characteristics to the physical properties of soils. *Water Resour. Res.,* **20,** 682–690.

Deardorff, J. W., 1978: Efficient prediction of ground surface temperature and moisture with inclusion of a layer of vegetation. *J. Geophys. Res.,* **83** (C4), 1889–1903.

de Vries, D. A., 1975: Heat transfer in soils. *Transfer Processes in the Plant Environment,* Part 1, *Heat and Mass Transfer in the Biosphere,* D. A. de Vries and N. H. Afgan, Eds., John Wiley and Sons, 4–28.

Ek, M., and R. H. Cuenca, 1994: Variation in soil parameters: Implications for modeling surface fluxes and atmospheric boundary-layer development. *Bound.-Layer Meteor.,* **70,** 369–383.

Hillel, D., 1980: *Fundamentals of Soil Physics.* Academic Press, 413 pp.

Jazwinski, A. H., 1970: *Stochastic Processes and Filtering Theory.* Academic Press, 376 pp.

Jia, P., and Z. Zhu, 1984: *Optimal Estimation and its Application* (in Chinese). Chinese Academic Press, 313 pp.

Koorevaar, P., G. Menelik, and C. Dirksen, 1983: *Elements of Soil Physics.* Elsevier, 228 pp.

Mancini, M., R. Hoeben, and P. A. Troch, 1999: Multifrequency radar observations of bare surface soil moisture content: A laboratory experiment. *Water Resour. Res.,* **35,** 1827–1838.

McCumber, M. C., and R. A. Pielke, 1981: Simulation of effects of surface fluxes of heat and moisture in a mesoscale numerical model. *J. Geophys. Res.,* **86** (C10), 9929–9938.

Mehra, R. K., 1972: Approaches to adaptive filtering. *IEEE Trans. Autom. Control,* **10,** 693–698.

Milly, P. C. D., 1982: Moisture and heat transport of hysteretic, inhomogeneous porous media: A matric head-based formulation and a numerical model. *Water Resour. Res.,* **18,** 489–498.

Montaldo, N., and J. D. Albertson, 2003: Multi-scale assimilation of surface soil moisture data for robust root zone moisture predictions. *Adv. Water Resour.,* **26,** 33–44.

Parlange, M. B., G. G. Katul, R. H. Cuenca, M. L. Kavvas, D. R. Nielsen, and M. Mata, 1992: Physical basis for a time series model of soil water content. *Water Resour. Res.,* **28,** 2437–2446.

——, ——, M. V. Folegatti, and D. R. Nielsen, 1993: Evaporation and the field scale water diffusivity function. *Water Resour. Res.,* **29,** 1279–1286.

Peters-Lidard, C. D., E. Blackburn, X. Liang, and E. F. Wood, 1998: The effect of soil thermal conductivity parameterization on surface energy fluxes and temperatures. *J. Atmos. Sci.,* **55,** 1209–1224.

Pielke, R. A., 1984: *Mesoscale Meteorological Modeling.* Academic Press, 612 pp.

Reece, C. F., 1996: Evaluation of a line heat dissipation sensor for measuring soil matric potential. *Soil Sci. Soc. Amer. J.,* **60,** 1022–1028.

Schneider, J. M., D. K. Fisher, R. L. Elliott, G. O. Browen, and C. P. Bahrmann, 2003: Spatiotemporal variation in soil water: First results from the ARM SGP CART network. *J. Hydrometeor.,* **4,** 106–120.

Starks, P. J., and T. J. Jackson, 2001: Remote sensing and estimation of root zone water content. *Remote Sensing and Hydrology 2000,* M. Owe et al., Eds., IAHS Publication 267, 409–411.

Ungar, S. G., R. Layman, J. E. Campbell, J. Walsh, and H. J. McKim, 1992: Determination of soil moisture distribution from impedance and gravimetric measurements of soil moisture in FIFE. *J. Geophys. Res.,* **97,** 18 979–18 985.

Van Geer, F. C., C. B. M. Te Stroet, and Y. Zhou, 1991: Using Kalman filtering to improve and quantify the uncertainty of numerical groundwater simulations: 1. The role of system noise and its calibration. *Water Resour. Res.,* **27,** 1987–1994.

Versteeg, H. K., and W. Malalasekera, 1995: *An Introduction to Computational Fluid Dynamics.* Longman Group, 257 pp.

Viterbo, P., and A. C. M. Beljaars, 1995: An improved land surface parameterization scheme in the ECMWF model and its validation. *J. Climate,* **8,** 2716–2748.

Xu, Q., and B. Zhou, 2003: Retrieving soil moisture from soil temperature measurements by using linear regression. *Adv. Atmos. Sci.,* **20,** 849–858.

——, ——, S. D. Burk, and E. H. Barker, 1999: An air–soil layer coupled scheme for computing surface heat fluxes. *J. Appl. Meteor.,* **38,** 211–223.

Zhou, B., and Q. Xu, 1999: Computing surface fluxes from Mesonet data. *J. Appl. Meteor.,* **38,** 1370–1383.